The 2017 World Congress on
Advances in Structural Engineering and Mechanics (ASEM17)
Ilsan(Seoul), Korea, August 28 - September 1, 2017

Keynote Paper

Topology Optimization of Structures subjected to Stochastic Dynamic Loading

Fernando Gomez[1)] and *Billie F. Spencer, Jr.[2)]

[1), 2)] *Department of Civil and Environmental Engineering, University of Illinois at Urbana-Champaign, 205 North Mathews Avenue, MC-250, Urbana, IL 61801, USA*
[2)] *bfs@illinois.edu*

ABSTRACT

Topology optimization has progressed substantially in recent years. Numerous papers have been written, with more and more results making their way into structural designs. However, the literature on topology optimization for structures subject to stochastic dynamic loads is limited. Most current approaches use Monte Carlo Simulation or replace the dynamic loads with a static or harmonic equivalent. In contrast, this study accounts directly for the stochastic nature of the excitation, modeling it as a zero-mean filtered white noise; when combined with the equations of motion for the structure, an augmented state space representation is formed. The objective function of the optimization is defined in terms of the covariances of the structural responses. Focusing on the stationary structural responses, the stochastic optimization problem is converted into its deterministic counterpart. To illustrate the framework, topology optimization of a rectangular domain, representing a mid-rise building under seismic excitation, is explored for a multi-objective performance function. These results are a first step toward efficient topology optimization of stochastically excited structures.

1. INTRODUCTION

Current structural design procedures are based on an iterative process, which guarantees structural safety but not optimal economy (Xu, et al. 2017). In this regard, topology optimization provides a general approach to obtain optimal material layout in a prescribed domain according to some cost function and subjected to given design constraints (Bendsøe and Sigmund 2003). Extensive research has been conducted in this field to develop well-posed formulations (Bendsøe and Kikuchi 1988, Sigmund and Petersson 1998, Sigmund 2007) and to solve the numerical problems generated by this approach, such as mesh dependency, checkerboarding, islanding, and local minima (Diaz and Sigmund 1995, Sigmund and Petersson 1998).

[1)] Doctoral Candidate
[2)] Nathan M. and Anne M. Newmark Endowed Chair in Civil Engineering

Topology optimization has been successfully applied to solve the minimum compliance problem subjected to deterministic static loading for general structures (Bendsøe and Sigmund 2003, Talischi, et al. 2012), as well as buildings (Stromberg, et al. 2012). It also has been applied to dynamic problems such as eigen-frequency optimization for free vibration (Olhoff 1989) and minimum dynamic compliance for forced harmonic vibration (Ma, et al. 1995). However, such deterministic approaches cannot accommodate stochastic dynamic loads which civil structures frequently undergo (e. g., winds, earthquakes, traffic, etc.; see Soong and Grigoriu 1993), and therefore, produce suboptimal designs.

Structural optimization of stochastically loaded structures has been slower to develop than its deterministic counterpart. Most of the research has been done in size optimization using Monte Carlo Simulation (Balling, et al. 2009; Allahdadian and Boroomand 2016). Recently, Chun, et al. (2016) proposed a reliability-based topology optimization approach for a Gaussian stationary stochastic excitation, using a discrete representation of the excitation and obtaining solution in the time-domain. These approaches are computationally expensive and convergence is only obtained in a statistical sense. Xu, et al. (2017a,b) proposed a structural optimization method for linear and nonlinear structures subjected to both stationary and nonstationary stochastic excitation; the performance function was formulated in terms of the response covariances, which were obtained through solution of the Lyapunov equation (Soong and Grigoriu 1993).

Directly applying the approach in Xu, et al. (2017a,b) to topology optimization results in large-scale problems for which traditional solution of the Lyapunov equation is intractable. Solution of the Lyapunov equation (i.e., $\mathbf{AX} + \mathbf{XA}^{\mathrm{T}} + \mathbf{Q} = \mathbf{0}$) is typically obtained using the Bartels-Steward or the Hessenberg-Schur algorithms (Golub, et al. 1979), which require the Schur decomposition of the matrix $\mathbf{A}$. These methods generally provide good results; however, the cubic time complexity and quadratic memory complexity impose a constraint on the size of problems that can be considered (Kressner 2008). Due to the low-rank nature of the matrix $\mathbf{Q}$, other techniques has been developed, including Krylov subspace methods (Saad 1990), matrix sign function decomposition with Newton's method (Higham 2008), and associated variations. These methods typically fail when the symmetric part of $\mathbf{A}$ is not negative definite (Benner, et al. 2008), which is the case in this study. In addition, the Alternating Direction Implicit (ADI) iteration algorithm was adapted to solve the Lyapunov equation with general $\mathbf{A}$ and low-rank $\mathbf{Q}$ (Penzl 1999, Benner, et al. 2008), which makes it an attractive option for the solution of large-scale Lyapunov equations found in topology optimization of structures subjected to stochastic dynamic loading.

This study proposes a topology optimization framework for stochastically excited structures, using a performance function in terms of the covariance of the stationary structural responses, obtained by solving a large-scale Lyapunov equation. An adjoint method is used to obtain the sensitivities of the performance function, which allows the use of efficient gradient-based updating procedures. Illustrative examples are provided for the optimization of a mid-rise building subjected to a stochastic ground motion using drifts-based and acceleration-based performance functions. The results demonstrate the efficacy of the proposed approach for multi-objective topology optimization of

stochastically excited structures.

2. STOCHASTIC EXCITATION AND RESPONSE

This section formulates the equations of motion as a state space representation, and models the input excitation as a filtered white noise. An augmented state space representation is then formed, and the stationary covariance of the responses are obtained via solution of the Lyapunov equation.

2.1 Equation of Motion and State Space Representation

The equation of motion (EOM) of an arbitrary N-degree-of-freedom linear system is given by

$$\mathbf{M}\ddot{\mathbf{u}} + \mathbf{C}\dot{\mathbf{u}} + \mathbf{K}\mathbf{u} = \mathbf{G}\mathbf{f}(t) \tag{1}$$

where $\mathbf{M}$ is the mass matrix; $\mathbf{C}$ is the damping matrix; $\mathbf{K}$ is the stiffness matrix; $\mathbf{u}$ is the displacement vector; $\mathbf{f}(t)$ is the input excitation vector; and $\mathbf{G}$ is the load-effect matrix. In topology optimization, these matrices are typically obtained using a Galerkin finite element approximation with first order shape functions. The input excitation vector, $\mathbf{f}(t)$ is assumed to be a stationary stochastic process.

Defining the state vector as

$$\mathbf{x} = \begin{bmatrix} \mathbf{u}^{\mathrm{T}} & \dot{\mathbf{u}}^{\mathrm{T}} \end{bmatrix}^{\mathrm{T}} \tag{2}$$

the state space representation of the system is given by

$$\begin{aligned} \dot{\mathbf{x}} &= \mathbf{A}_{\mathrm{s}}\mathbf{x} + \mathbf{B}_{\mathrm{s}}\mathbf{f}(t) \\ \mathbf{y} &= \mathbf{C}_{\mathrm{s}}\mathbf{x} + \mathbf{D}_{\mathrm{s}}\mathbf{f}(t) \end{aligned} \tag{3}$$

where the matrices $\mathbf{A}_{\mathrm{s}}$ and $\mathbf{B}_{\mathrm{s}}$ are given by

$$\mathbf{A}_{\mathrm{s}} = \begin{bmatrix} \mathbf{0}_{N\times N} & \mathbf{I}_{N\times N} \\ -\mathbf{M}^{-1}\mathbf{K} & -\mathbf{M}^{-1}\mathbf{C} \end{bmatrix}, \quad \mathbf{B}_{\mathrm{s}} = \begin{bmatrix} \mathbf{0}_{N\times 1} \\ \mathbf{M}^{-1}\mathbf{G} \end{bmatrix} \tag{4}$$

and the matrices $\mathbf{C}_{\mathrm{s}}$ and $\mathbf{D}_{\mathrm{s}}$ depend on the desired output $\mathbf{y}$.

2.2 Stochastic Excitation Model

In this study, the excitation is assumed as a zero-mean stationary stochastic process that can be modeled as a filtered white noise, admitting the following state space representation

$$\begin{aligned} \dot{\mathbf{x}}_{\mathrm{g}} &= \mathbf{A}_{\mathrm{g}}\mathbf{x}_{\mathrm{g}} + \mathbf{B}_{\mathrm{g}}\mathbf{w}(t) \\ \mathbf{f} &= \mathbf{C}_{\mathrm{g}}\mathbf{x}_{\mathrm{g}} \end{aligned} \tag{5}$$

where $\mathbf{x}_{\mathrm{g}}$ is the state vector of the excitation; the matrices $\mathbf{A}_{\mathrm{g}}$, $\mathbf{B}_{\mathrm{g}}$, and $\mathbf{C}_{\mathrm{g}}$ are determined

by the characteristics of the excitation; and $\mathbf{w}(t)$ is a multi-dimensional white noise described by

$$\mathbb{E}(\mathbf{w}(t)) = 0, \quad \mathbb{E}(\mathbf{w}(t_1)\mathbf{w}(t_2)) = 2\pi\mathbf{S}_0\delta(t_1 - t_2) \tag{6}$$

where $\mathbb{E}(\cdot)$ is the expected value operator; $\mathbf{S}_0$ as the constant two-sided power spectral density matrix of the noise; and $\delta(\cdot)$ is the Dirac delta function.

Defining the augmented state vector as

$$\mathbf{x}_\mathrm{a} = \begin{bmatrix}\mathbf{x}^\mathrm{T} & \mathbf{x}_\mathrm{g}^\mathrm{T}\end{bmatrix}^\mathrm{T} \tag{7}$$

then the augmented system is given as

$$\begin{aligned}\dot{\mathbf{x}}_\mathrm{a} &= \mathbf{A}_\mathrm{a}\mathbf{x}_\mathrm{a} + \mathbf{B}_\mathrm{a}\mathbf{w}(t)\\ \mathbf{y} &= \mathbf{C}_\mathrm{a}\mathbf{x}_\mathrm{a}\end{aligned} \tag{8}$$

where the matrices $\mathbf{A}_\mathrm{a}$, $\mathbf{B}_\mathrm{a}$, and $\mathbf{C}_\mathrm{a}$ are

$$\mathbf{A}_\mathrm{a} = \begin{bmatrix}\mathbf{A}_\mathrm{s} & \mathbf{B}_\mathrm{s}\mathbf{C}_\mathrm{g}\\ \mathbf{0}_{N_g\times N} & \mathbf{A}_\mathrm{g}\end{bmatrix}, \quad \mathbf{B}_\mathrm{a} = \begin{bmatrix}\mathbf{0}_{2N\times 1}\\ \mathbf{B}_\mathrm{g}\end{bmatrix}, \quad \mathbf{C}_\mathrm{a} = \begin{bmatrix}\mathbf{D}_\mathrm{s}\mathbf{C}_\mathrm{g} & \mathbf{C}_\mathrm{s}\end{bmatrix}. \tag{9}$$

2.3 Stochastic Structural Response

The covariance matrix of the vector $\mathbf{x}_\mathrm{a}$ is defined as

$$\mathbf{\Gamma}_{\mathbf{x}_\mathrm{a}} = \mathbb{E}((\mathbf{x}_\mathrm{a} - \mu_{\mathbf{x}_\mathrm{a}})(\mathbf{x}_\mathrm{a} - \mu_{\mathbf{x}_\mathrm{a}})^\mathrm{T}) \tag{10}$$

Because the excitation is a zero-mean process, then the response is also a zero-mean process; consequently the covariance of the response is given by

$$\mathbf{\Gamma}_{\mathbf{x}_\mathrm{a}} = \mathbb{E}(\mathbf{x}_\mathrm{a}\mathbf{x}_\mathrm{a}^\mathrm{T}) \tag{11}$$

The covariance of the stationary response of the augmented state is governed by the Lyapunov equation

$$\mathbf{A}_\mathrm{a}\mathbf{\Gamma}_{\mathbf{x}_\mathrm{a}} + \mathbf{\Gamma}_{\mathbf{x}_\mathrm{a}}\mathbf{A}_\mathrm{a}^\mathrm{T} + 2\pi\mathbf{B}_\mathrm{a}\mathbf{S}_0\mathbf{B}_\mathrm{a}^\mathrm{T} = \mathbf{0} \tag{12}$$

and the covariance of the system output $\mathbf{y}$ is given by

$$\mathbf{\Gamma}_\mathbf{y} = \mathbb{E}(\mathbf{y}\mathbf{y}^\mathbf{T}) = \mathbf{C}_\mathrm{a}\mathbf{\Gamma}_{\mathbf{x}_\mathrm{a}}\mathbf{C}_\mathrm{a}^\mathrm{T}. \tag{13}$$

Because the matrix $\mathbf{A}_\mathrm{a}$ is Hurwitz, and the matrix $2\pi\mathbf{B}_\mathrm{a}\mathbf{S}_0\mathbf{B}_\mathrm{a}^\mathrm{T}$ given in the last term of Eq. (12) is positive semidefinite, the solution for $\mathbf{\Gamma}_\mathbf{y}$ is unique and positive semidefinite.

3. PROBLEM FORMULATION AND SOLUTION

This section summarizes the topology optimization framework for structures subjected to stochastic excitations proposed in (Gomez and Spencer 2017), including the objective function and the constraints. The details of the topology optimization solution process are also presented.

3.1 Topology Optimization Formulation

The topology optimization is based on intermediate element densities (Bendsøe and Sigmund 2003), such that for each element, a relative density variable ***z*** is chosen. SIMP interpolation is used for the Young's modulus and density for each element, which yields

$$\begin{aligned} E(z) &= [\epsilon + (1-\epsilon)z^p]E^0 \\ \rho(z) &= [\epsilon + (1-\epsilon)z^q]\rho^0 \end{aligned} \tag{14}$$

where E^0 and ρ^0 are the Young's modulus and density for the solid material, p and q are the penalization factors, and ϵ is a small number.

The optimization formulation is given by finding the vector of density variables **z**,

$$\begin{aligned} \min_{\mathbf{z}} \; & J(\mathbf{z}) = \mathbf{F}(\mathbf{z}) : \mathbf{\Gamma}_{\mathbf{x}_\mathrm{a}}(\mathbf{z}) \\ \text{s.t.} \; & g(\mathbf{z}) = V(\mathbf{z}) - V_{\max} \leq 0 \\ & \mathbf{A}_\mathrm{a}\mathbf{\Gamma}_{\mathbf{x}_\mathrm{a}} + \mathbf{\Gamma}_{\mathbf{x}_\mathrm{a}}\mathbf{A}_\mathrm{a}^\mathrm{T} + 2\pi\mathbf{B}_\mathrm{a}\mathbf{S}_0\mathbf{B}_\mathrm{a}^\mathrm{T} = \mathbf{0} \\ & z_n \in [z_{\min}, z_{\max}] \text{ for } n = 1, 2, \ldots, N \end{aligned} \tag{15}$$

where : represents the double dot product between matrices, $\mathbf{F}$ is a symmetric positive semidefinite matrix, V is the volume, $V_{\max}$ is the volume limit, and $z_{\min}$ and $z_{\max}$ are the lower and upper bounds on the density variables. Note that the proposed performance function allows many types of responses (e.g., displacements, drifts, accelerations) of one or many points; and that the performance function is completely defined by the covariance of the response.

As indicated previously, the covariance of the response of the structure subjected to a stochastic process is obtained by solving the Lyapunov equation in Eq. (12), and consequently, the topology optimization problem is deterministic. Fig. 1 shows the flowchart for the solution procedure of the optimization problem. The remainder of this section details the respective steps in this procedure.

3.2 Lyapunov Equation Solver

The Lyapunov equation Eq. (12) can be rewritten as

$$\mathbf{A}_\mathrm{a}\mathbf{\Gamma}_{\mathbf{x}_\mathrm{a}} + \mathbf{\Gamma}_{\mathbf{x}_\mathrm{a}}\mathbf{A}_\mathrm{a}^\mathrm{T} + \tilde{\mathbf{B}}_\mathrm{a}\tilde{\mathbf{B}}_\mathrm{a}^\mathrm{T} = \mathbf{0} \tag{16}$$

where $\mathbf{A}_{\mathrm{a}}$ is a $N\times N$ matrix; $\tilde{\mathbf{B}}_{\mathrm{a}}=\sqrt{2\pi}\tilde{\mathbf{S}}$ is an $N\times m$ matrix with m much smaller than

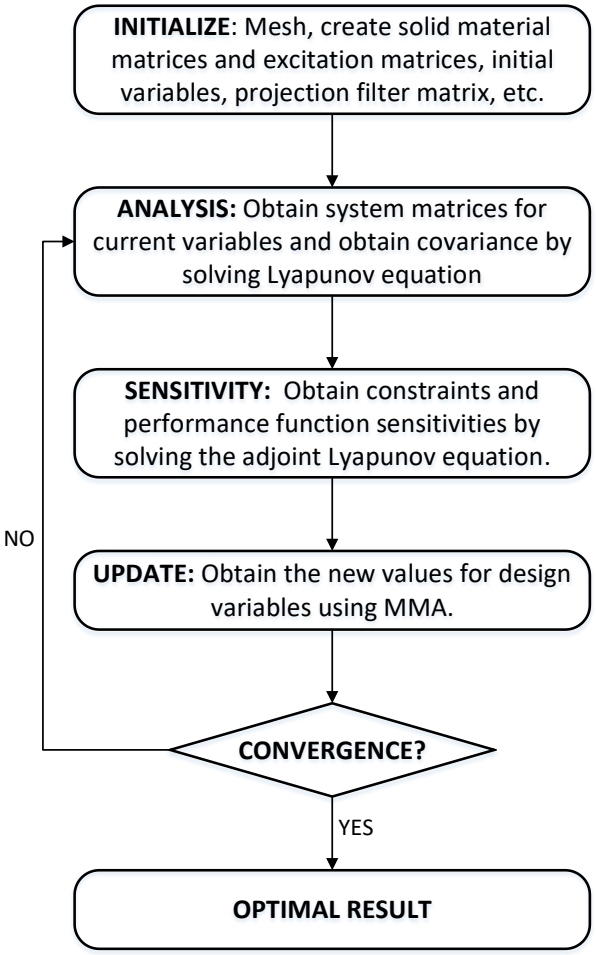

Fig. 1 Topology optimization flowchart for stochastically excited structures

N; and $\tilde{\mathbf{S}}$ is the lower Cholesky factor of $\mathbf{S}_0$. The Cholesky factor ADI iterative algorithm is applied to obtain the complex matrix $\mathbf{Z}$ (Benner, et al. 2008) such that $\mathbf{\Gamma}_{\mathbf{x}_{\mathrm{a}}}=\mathbf{Z}\mathbf{Z}^{\mathrm{H}}$ where

$$\mathbf{Z}=\begin{bmatrix}\mathbf{V}_1 & \mathbf{V}_2 & \dots & \mathbf{V}_n\end{bmatrix} \tag{17}$$

and the matrices $\mathbf{V}_i$ are obtained using the iterative procedure showed in the following equations

$$\begin{aligned}\mathbf{V}_1&=\sqrt{-2\Re(p_1)}(\mathbf{A}_{\mathrm{a}}+p_1\mathbf{I})^{-1}\tilde{\mathbf{B}}_{\mathrm{a}}\\ \mathbf{V}_k&=\sqrt{\frac{\Re(p_k)}{\Re(p_{k-1})}}[\mathbf{V}_{k-1}-(p_k+\bar{p}_{k-1})(\mathbf{A}_{\mathrm{a}}+p_k\mathbf{I})^{-1}\mathbf{V}_{k-1}]\end{aligned} \tag{18}$$

where the overscore denotes the complex conjugate, p_i are complex shift parameters with negative real parts that satisfy the following minimax problem

$$\{p_1, p_2, \ldots, p_l\} = \arg \min_{\{p_1,\ldots,p_l\}\in\mathbb{C}^-} \max_{t\in\sigma(\mathbf{A}_a)} \frac{|r_l(t)|}{|r_l(-t)|}$$
$$r_l(t) = \prod_{i=1}^{l}(t - p_i) \tag{19}$$

where $\sigma(\mathbf{A}_a)$ denotes the spectrum of $\mathbf{A}_a$. The algorithm proposed by Penzl (1999) to obtain a set of sub-optimal parameters is used.

The accuracy and efficiency of the method depend on 4 parameters: k^+ is the number of Ritz values using power iteration, k^- is the number of Ritz values using inverse iteration, l is the number of parameters, and n is the number of iterations. A numerical test of a 5 x 15 rectangular domain discretized into 7500 elements can show the convergence and accuracy of the method. The residual of the Lyapunov equation is defined as

$$\mathbf{R} = \mathbf{A}_a\mathbf{\Gamma}_{\mathbf{x}_a} + \mathbf{\Gamma}_{\mathbf{x}_a}\mathbf{A}_a^T + \tilde{\mathbf{B}}_a\tilde{\mathbf{B}}_a^T. \tag{20}$$

Fig. 2 shows the convergence of the logarithm using the Frobenius norm of the residual $\mathbf{R}$ while varying the number of iterations and the number of parameters for a fixed number of Ritz values (k^+ = 50, k^- = 25). The error norm approaches zero as the number of iterations is increased.

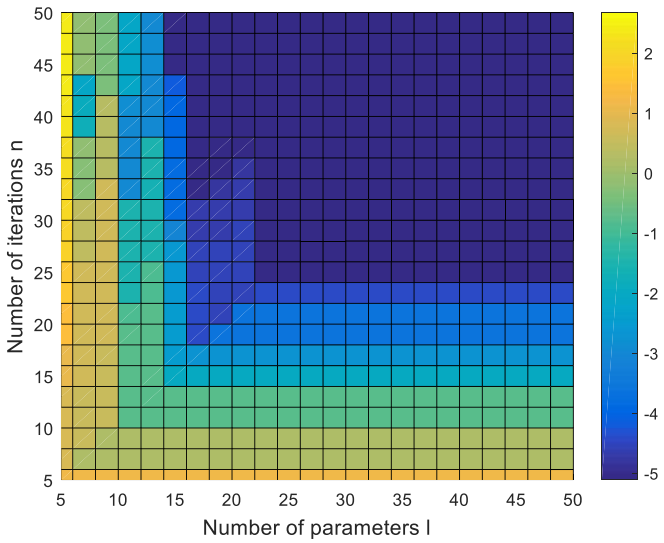

Fig. 2 Convergence of the log of the Frobenius norm of the residual of Eq. (16)

3.3 Sensitivity Analysis

The gradient of the performance function and constraints are required to use the chosen updating procedure, which is the the method of moving asymptotes (Svanberg 1987). The performance function defined in Eq. (15) depends on the covariance matrix, which is implicitly defined by Eq. (12); hence, an adjoint method is implemented to

eliminate implicitly defined gradients and reduce computational time (Gomez and Spencer 2017).

The sensitivity of the performance function is given by the following equation

$$\frac{\partial J}{\partial z_n} = \left(\frac{\partial \mathbf{A}_\mathrm{a}}{\partial z_n}\mathbf{\Gamma}_{\mathbf{x}_\mathrm{a}} + \mathbf{\Gamma}_{\mathbf{x}_\mathrm{a}}\frac{\partial \mathbf{A}_\mathrm{a}^\mathrm{T}}{\partial z_n} + \frac{\partial(\tilde{\mathbf{B}}_\mathrm{a}\tilde{\mathbf{B}}_\mathrm{a}^\mathrm{T})}{\partial z_n}\right) : \mathbf{\Lambda} + \frac{\partial \mathbf{F}}{\partial z_n} : \mathbf{\Gamma}_{\mathbf{x}_\mathrm{a}} \tag{21}$$

where the sensitivities of the performance function require the derivatives of the matrices $\mathbf{A}_\mathrm{a}$, $\mathbf{B}_\mathrm{a}$, and $\mathbf{F}$ that were explicitly defined in previous sections; and the Lagrange multiplier matrix $\mathbf{\Lambda}$, which is symmetric and positive semidefinite, is obtained by solving the adjoint Lyapunov equation

$$\mathbf{A}_\mathrm{a}^\mathrm{T}\mathbf{\Lambda} + \mathbf{\Lambda}\mathbf{A}_\mathrm{a} + \mathbf{F} = \mathbf{0} \tag{22}$$

Note that $\mathbf{F}$ can be expressed as a low-rank matrix product, hence, the algorithm described in section 3.2 also can be applied here.

A numerical test of a rectangular domain of 5 x 15 discretized into 300 elements shows the accuracy of the method. Fig. 3 provides a comparison of the sensitivities of the covariance of the top lateral displacement with respect to each element variable using the adjoint and finite difference method. As these figures demonstrate, the proposed adjoint method accurately computes the sensitivities. Also, note that the adjoint method reduces time complexity, because the total number of Lyapunov equations to be solved is reduced, admitting use of the CF-ADI solver.

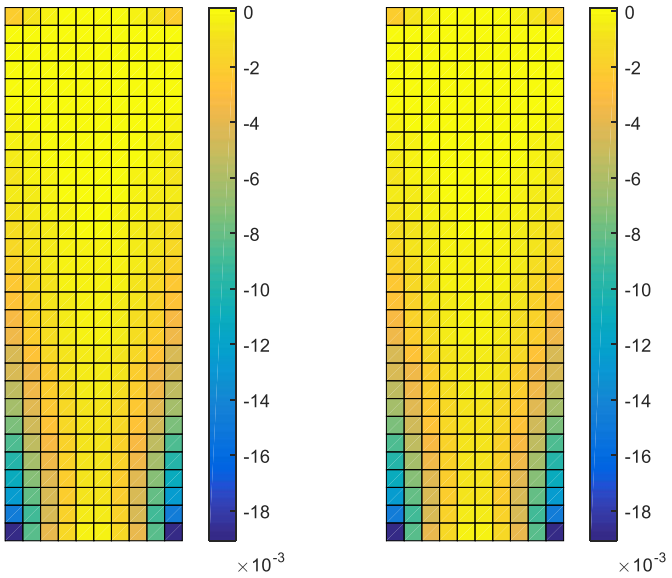

Fig. 3 Sensitivity of the covariance of the top lateral displacement using adjoint method (left) and finite difference method (right)

4. ILLUSTRATIVE EXAMPLES

In this section, the proposed framework is illustrated through examples optimizing the lateral force resisting system of a building subjected to a seismic ground motion in the horizontal direction. In the equation of motion, **G** is the load-effect vector, which has components equal to 1 only for the DOFs in the direction of the ground motion, **u** is the relative displacement to the ground, and f is the scalar stochastic ground acceleration. The design domain is a 5 x 15 rectangle, which is depicted in Fig. 4. This domain is first optimized to minimize lateral interstory drift; subsequently, a Pareto optimization approach is employed to explore the tradeoffs between minimizing the lateral interstory drifts and lateral absolute accelerations, which are competing objectives (Xu, et al. 2017).

The solid linear elastic material has the following properties: Young's modulus E^0 =210 GPa, Poisson's ratio $\nu = 0.3$, density $\rho = 2400$ kg/m^3, and Ersatz parameter $\epsilon = 10^{-4}$. The domain has an uniform thickness of 0.10 m; to achieve more realistic topologies (Stromberg, et al. 2012), the domain is bounded by 0.40 x 0.40 columns with the same material properties; the continuum domain is assumed to be in plane stress. The continuum domain is discretized using 7500 Q4 elements, and the boundary columns are discretized using 180 frame elements such that their nodes coincide with the nodes of the Q4 elements. Two additional floor lumped masses of 6000 kg are included at each floor to simulate floor mass (see red dots in Fig. 4), which is equivalent to 20 times the total allowable mass of the design domain. The radius of the projection filter is equal to 0.35.

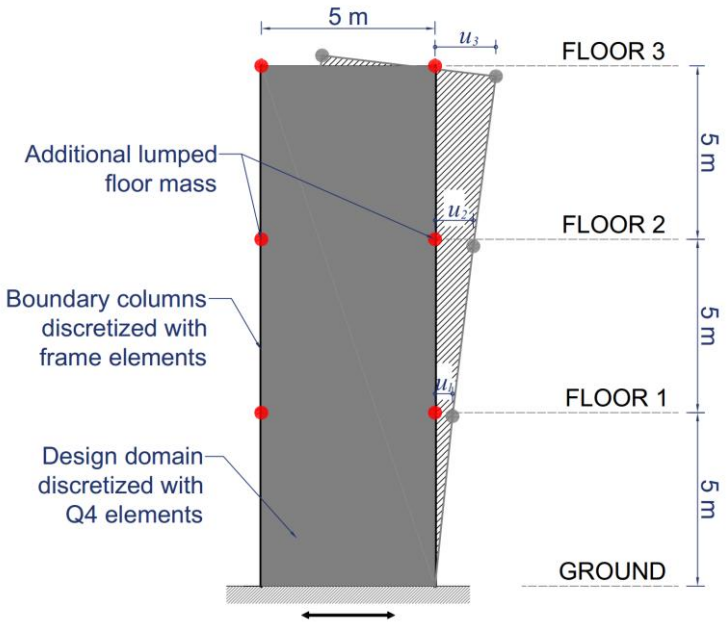

Fig. 4 Rectangular domain geometry for the numerical examples

The ground motion is modeled using a Kanai-Tajimi spectrum with S_0 = 1; the space state matrices are

$$\mathbf{A}_{\mathrm{g}} = \begin{bmatrix} 0 & 1 \\ -\omega_{\mathrm{g}}^2 & -2\omega_{\mathrm{g}}\zeta_{\mathrm{g}} \end{bmatrix}, \quad \mathbf{B}_{\mathrm{g}} = \begin{bmatrix} 0 \\ 1 \end{bmatrix}, \quad \mathbf{C}_{\mathrm{g}} = \begin{bmatrix} \omega_{\mathrm{g}}^2 & 2\omega_{\mathrm{g}}\zeta_{\mathrm{g}} \end{bmatrix} \tag{23}$$

where ω_{g} and ζ_{g} are the natural frequency and damping ratio of the ground excitation model, respectively. $\omega_{\mathrm{g}} = 20.3$ rad/s and $\zeta_{\mathrm{g}} = 0.32$ are chosen in the first example corresponding to the average values of 140 earthquake records (Lai 1982).

4.1 Drift Optimization of a 3-Story Building

In this example, the sum of the covariance of the lateral interstory drifts is minimized. The performance function chosen for this optimization is given by

$$J_{\mathrm{d}}(\mathbf{z}) = \sum_{i=1}^{N_{\mathrm{f}}} \mathbb{E}(\Delta u_i^2) \tag{24}$$

where Δu_i is the lateral interstory drift of the i^{th} floor. The matrix $\mathbf{F}$ can be rewritten as $\mathbf{C}\mathbf{C}^{\mathrm{T}}$, where $\mathbf{C}$ is an $N_{\mathrm{f}} \times N$ matrix whose i^{th} row has a 1 in the i^{th} floor lateral displacement DOF, -1 in the $i-1^{\mathrm{th}}$ floor lateral displacement DOF, and the other entries are zeros. The volume is constrained to be less or equal than 0.30 of the solid domain.

The results in Fig. 5 show the convergence of the performance function and that the volume constraint is enforced. The optimal topology for interstory drift optimization is composed of 3 pairs of braces with stiffness inversely proportional to height, which coincide with engineering intuition. This result is consistent with the results obtained by Xu, et al. (2017) for parametric optimization of shear building subjected to stochastic ground motions. Also, note that for the bottom brace, the intersection point is not centered vertically. Additionally, the first and second frequencies are 29.6 rad/s and 86.5 rad/s, respectively; which are far from the dominant excitation frequency of 20 rad/s.

4.2 Pareto Optimal Front of a 3-Story Building

Xu et al. (2017a,b) showed that the interstory drift and absolute acceleration are competing objectives for seismically excited structures. Therefore, the Pareto optimal curve is introduced to explore the tradeoffs between these two objectives. A combined performance function is defined as

$$J_{\alpha}(\mathbf{z}) = (1-\alpha)\bar{J}_{\mathrm{d}}(\mathbf{z}) + \alpha\bar{J}_{\mathrm{a}}(\mathbf{z}) \tag{25}$$

where

$$J_{\mathrm{a}}(\mathbf{z}) = \sum_{i=1}^{N_{\mathrm{f}}} \mathbb{E}(\ddot{u}_{\mathrm{a},i}^2) \tag{26}$$

α is the weighting parameter between 0 and 1, and the overbar indicates that the performance function is normalized by the minimum in the respective single-objective functions, such that the performance function is dimensionless. When $\alpha = 0$, the function represents the interstory drift objective, and when $\alpha = 1$, the function represents

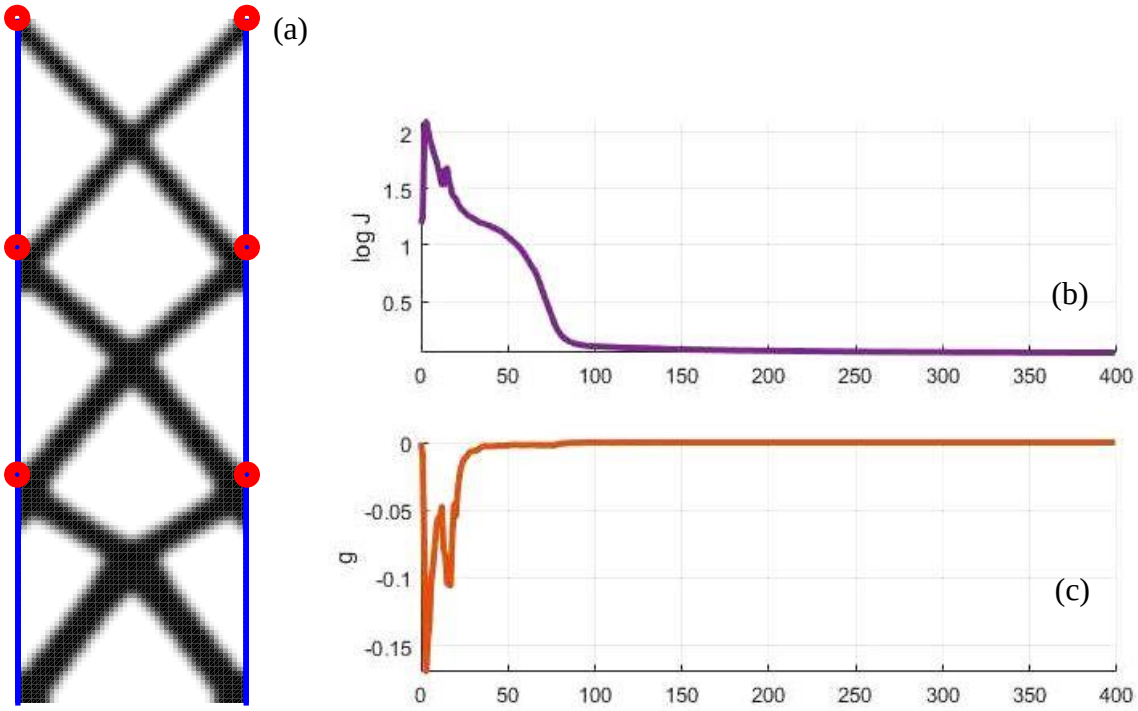

Fig. 5 Results for sum of covariance of interstory lateral drift function: a) optimal topology, b) performance function evolution, c) volume constraint evolution

the acceleration objective. The volume is constrained to be less or equal than 0.30 of the solid domain.

In this example, the excitation is given by a white noise to provide uniform excitation to all frequencies. Fig. 6 shows the results for the topology optimization for two different values of α. As expected, as α increases, the topology transitions from the interstory drift objective to the acceleration objective: more stiffness and mass is allocated in the top floor and stiffness in the lower floors is reduced. Note that as α increases, the braces do not necessarily meet at the floors.

Fig. 7 shows the Pareto optimal front for this example, the x-axis represents the ratio of the maximum interstory drift standard deviation and the maximum interstory drift standard deviation for $\alpha = 0$, and the y-axis represents the ratio of the maximum floor acceleration standard deviation and the maximum floor acceleration standard deviation for $\alpha = 1$. All the points below the curve correspond to infeasible designs.

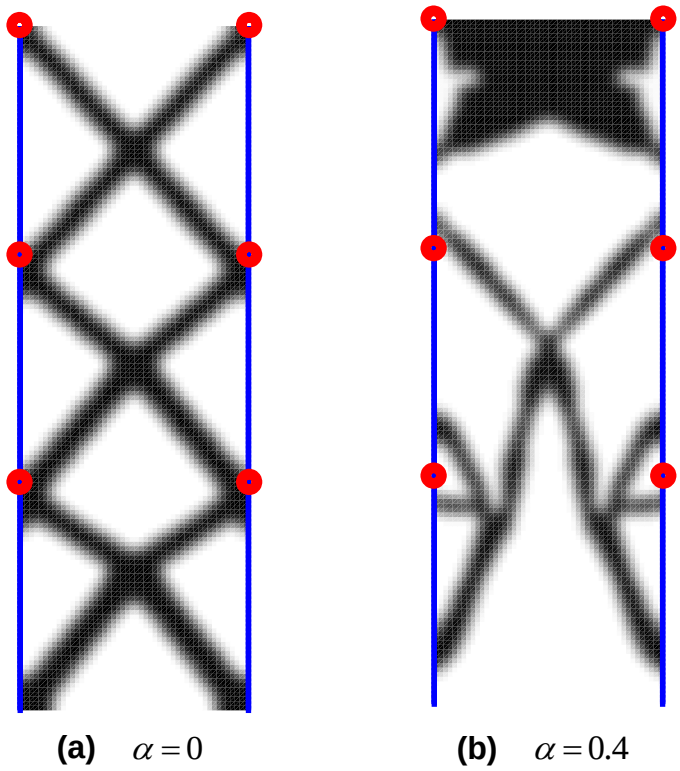

Fig. 6 Topology optimization of the Pareto combination of the drift and acceleration performance objectives

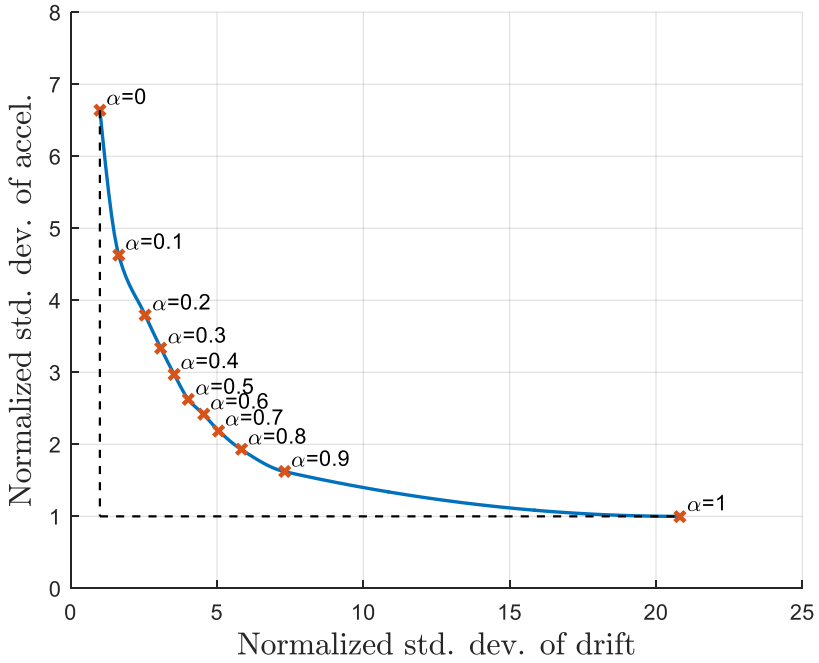

Fig. 7 Pareto optimal front of the example

5. CONCLUSIONS

This paper presented a multi-objective framework for topology optimization of stochastically excited structures. The input was modeled as a filtered white noise, and the performance of the structure due to this excitation was given in terms of the covariance of the stationary structural responses. The objective function for the optimization was defined as the trace of the product of a positive semidefinite symmetric and the covariance of the stationary response. The covariances were obtained by solving a large-scale Lyapunov equation using an algorithm which is efficient both in terms of memory and computational time. The objective function was shown to be general enough to represent displacement, interstory drifts, velocities, and accelerations at one or many points. A volume constraint was imposed to limit the design space, and the design variables were chosen as the relative densities in each element, which were bounded to achieve physically meaningful solutions. The material properties for intermediate densities were obtained using the SIMP interpolation rule; a linear hat projection filter was used to avoid numerical instabilities. The sensitivities of the performance function were obtained using an adjoint method, which requires the solution of an adjoint Lyapunov equation, also solved using the Lyapunov equation solver. Iterations were carried out using a gradient-based approach commonly employed in the topology optimization field.

The proposed framework was illustrated by conducting topology optimization for a rectangular domain meshed using 7500 Q4 elements, 180 frame elements in the lateral boundaries, and additional lumped floor masses, representing the lateral resisting system of a mid-rise building under stochastic earthquake loading. First, optimization was performed for the lateral interstory drift objective. The optimal topology was a system of 3 pairs of braces with stiffness inversely proportional to height. Subsequently, the trade-off between minimizing interstory drift and absolute floor acceleration, which are competing design objectives, was explored using Pareto optimal curve. To minimize acceleration, more stiffness was allocated in the top floor. These results demonstrate the efficacy of the proposed approach for multi-objective topology optimization of stochastically excited structures.

REFERENCES

Allahdadian, S., & Boroomand, B. (2016). “Topology optimization of planar frames under seismic loads induced by actual and artificial earthquake records,” *Engineering Structures*, ***115***, 140–154.

Balling, R. J., Balling, L. J., & Richards, P. W. (2009). “Design of Buckling-Restrained Braced Frames Using Nonlinear Time History Analysis and Optimization,” *Journal of Structural Engineering*, ***135***(5), 461–468

Bendsøe, M. P., & Kikuchi, N. (1988). “Generating optimal topologies in structural design using a homogenization method,” *Computer Methods in Applied Mechanics and Engineering*, ***71***(2), 197–224.

Bendsøe, M. P., & Sigmund, O. (2003). *Topology optimization: theory, methods, and applications*. Springer.

Benner, P., Li, J.-R., & Penzl, T. (2008). “Numerical solution of large-scale Lyapunov equations, Riccati equations, and linear-quadratic optimal control problems,” *Numerical Linear Algebra with Applications*, ***15***(9), 755–777.

Chun, J., Song, J., & Paulino, G. H. (2016). “Structural topology optimization under constraints on instantaneous failure probability,” *Structural and Multidisciplinary Optimization*, ***53***(4), 773–799.

Díaz, A., & Sigmund, O. (1995). “Checkerboard patterns in layout optimization,” *Structural Optimization*, ***10***(1), 40–45.

Golub, G., Nash, S., & Van Loan, C. (1979). “A Hessenberg-Schur method for the problem AX + XB= C,” *IEEE Transactions on Automatic Control*, ***24***(6), 909–913.

Gomez, F., & Spencer, B. F. (2017). “Topology optimization framework for structures subjected to stationary stochastic dynamic loads,” *Structural and Multidisciplinary Optimization*, Submitted.

Higham, N. J. (2008). *Functions of matrices: theory and computation*. Society for Industrial and Applied Mathematics

Kressner, D. (2008). “Memory-efficient Krylov subspace techniques for solving large-scale Lyapunov equations,” *2008 IEEE International Conference on Computer-Aided Control Systems* (pp. 613–618). IEEE.

Lai, S. P. (1982). “Statistical characterization of strong ground motions using power spectral density function,” *Bulleting of the Seismological Society of America*, ***72*****,** 259-274.

Ma, Z.-D., Kikuchi, N., & Cheng, H.-C. (1995). “Topological design for vibrating structures,” *Computer Methods in Applied Mechanics and Engineering*, ***121***(1–4), 259–280.

Olhoff, N. (1989). “Multicriterion structural optimization via bound formulation and mathematical programming,” *Structural Optimization*, ***1***(1), 11–17.

Penzl, T. (1999). “A Cyclic Low-Rank Smith Method for Large Sparse Lyapunov Equations,” *SIAM Journal on Scientific Computing*, ***21***(4), 1401–1418.

Saad, Y. (1990). “Numerical Solution of Large Lyapunov Equations,” *Signal processing, scattering and operator theory, and numerical methods, proc. MTNS-89*, ***3***, 503–511.

Sigmund, O. (2007). “Morphology-based black and white filters for topology optimization,” *Structural and Multidisciplinary Optimization*, ***33***(4–5), 401–424.

Sigmund, O., & Petersson, J. (1998). “Numerical instabilities in topology optimization: A survey on procedures dealing with checkerboards, mesh-dependencies and local minima,” *Structural Optimization*, ***16***(1), 68–75.

Soong, T. T., & Grigoriu, M. (1993). *Random vibration of mechanical and structural systems*. PTR Prentice Hall.

Stromberg, L. L., Beghini, A., Baker, W. F., & Paulino, G. H. (2012). “Topology optimization for braced frames: Combining continuum and beam/column elements,” *Engineering Structures*, ***37***, 106–124.

Svanberg, K. (1987). “The method of moving asymptotes—a new method for structural optimization,” *International Journal for Numerical Methods in Engineering*, ***24***(2), 359–373.

Talischi, C., Paulino, G. H., Pereira, A., & Menezes, I. F. M. (2012). “PolyTop: a Matlab implementation of a general topology optimization framework using unstructured

polygonal finite element meshes," *Structural and Multidisciplinary Optimization*, ***45***(3), 329–357.

Xu, J., Spencer, B. F., Lu, X., Chen, X., & Lu, L. (2017a). "Optimization of structures subject to stochastic dynamic loading." *Computer-Aided Civil and Infrastructure Engineering*, in press.

Xu, J., Spencer, B. F., & Lu, X. (2017b). "Performance-based optimization of nonlinear structures subject to stochastic dynamic loading," *Engineering Structures*, ***134***, 334–345.